Opt Quant Electron (2008) 40:217–226
DOI 10.1007/s11082-008-9219-4

Modeling of gain and phase dynamics in quantum dot amplifiers

Pablo Moreno · Marco Rossetti · Benoît Deveaud-Plédran · Andrea Fiore

Received: 21 August 2007 / Accepted: 20 May 2008 / Published online: 25 June 2008

Abstract By means of an electron hole rate equation model we explain the phase dynamics of a quantum dot semiconductor optical amplifier and the appearance of different decay times observed in pump and probe experiments. The ultrafast hole relaxation leads to a first ultrafast recovery of the gain, followed by electron relaxation and, in the nanosecond timescale, radiative and non-radiative recombinations. The phase dynamics is slower and is affected by thermal redistribution of carriers within the dot. We explain the ultrafast response of quantum dot amplifiers as an effect of hole escape and recombination without the need to assume Auger processes.

Keywords Electron-hole model · InAs · Phase dynamics · Quantum dot · Rate-equations · Semiconductor optical amplifiers

1 Introduction

Quantum dot (QD) materials have shown several breakthrough characteristics when compared to their quantum well counter-parts, such as broad gain (Rossetti et al. 2005), low chirp (Saito et al. 2000) or temperature independent threshold current (Fathpour et al. 2004). However, one of the most discussed features of QDs relates to their gain and phase dynamics. The phase dynamics is particularly interesting for understanding laser chirp and for application of QD amplifiers as phase modulators in all-optical Mach-Zehnder modulators (Uskov 2004). The existing pump and probe experiments (Borri et al. 2006; Cesari et al. 2007; Piwonski et al. 2007; Poel et al. 2005) show very slow phase recovery and several time constants in the gain and phase recovery, the fastest being subpicosecond. This fast time constant has been

P. Moreno (✉) · M. Rossetti · B. Deveaud-Plédran
Ecole Polytechnique Fédérale de Lausanne, EPFL/IPEQ/LOEQ, Station 3, 1015 Lausanne, Switzerland
e-mail: pablo.moreno@epfl.ch

A. Fiore
Photonics and Semiconductor Nanophysics, Eindhoven University of Technology, PO Box 513, d1-10 Eindhoven, The Netherlands

generally attributed to Auger mediated carrier capture for InAs (Piwonski et al. 2007) and InGaAs (Narvaez et al. 2006) active layers, through rate-equation excitonic models.

Despite the general acceptance of excitonic models to describe some of the quantum dot characteristics, electron-hole models have showed success explaining the L-I characteristics (Viktorov et al. 2005) and the temperature dependence of photoluminescence (Dawson et al. 2005) of QD devices. Recently, a simple model electron-hole model was used to reproduce gain measurements of two-color pump and probe experiments (O'Driscoll et al. 2007).

In this paper, we present a detailed electron-hole rate-equation model which gives qualitative and quantitative insight into the physics behind gain and phase dynamics of a QD gain medium. This model straight forwardly explains the ultrafast response of QD amplifiers as an effect of hole escape and recombination without the need to assume Auger processes.

2 Model

To properly describe the gain changes of the layer while taking into account the phase shift produced at the ground state (GS) energy, we consider the population of three different levels: the GS (two degenerated states), the first excited state (ES) within the dot (four degenerated states), and a 2D quantum well corresponding to the wetting layer (WL). In order to account for the inhomogeneous broadening and spectral distribution (Fig. 1) of carriers within the QD ensemble, we divide each energetic level into 100 different sections corresponding to different dot families with different energies, as done by Markus et al. (2005). We use a mean field model, neglecting spatial variations along the cavity.

The parameters used in the model correspond to the InAs/GaAs QD material system, with emission wavelength around 1,300 nm. We assume a Gaussian distribution of the transition energies with a full width half maximum (FWHM) of 35 meV, for both the ES and the GS,

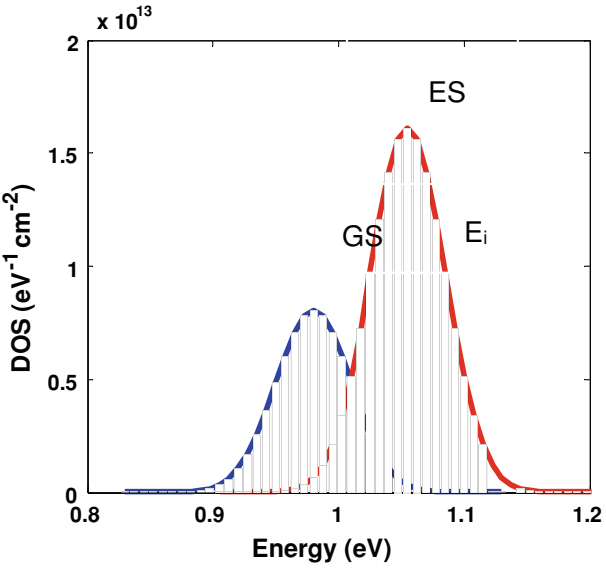

Fig. 1 Energy discretization of the GS and ES

obtained by low-temperature photoluminescence spectra (Markus et al. 2005). The GS is centered at 0.98 eV and the ES is centered at 1.055 eV.

If we take a certain energy interval $E_i \pm \Delta E_G$, the number of QDs with GS transition energies at this interval should be:

$$N^{GS(E_i)} = \frac{N_D}{\sqrt{2\pi\sigma}} \int_{E_i+\frac{\Delta E_{GS}}{2}}^{E_i+\frac{\Delta E_{GS}}{2}} \exp\left[\frac{-\left(E - E_{peak}^{GS}\right)^2}{2\sigma^2}\right] dE$$

where σ is related to the FWHM as $\sigma = FWHM \cdot 2\sqrt{2\ln 2}$, N_D is the dot areal density ($3\,10^{10}\,cm^{-2}$) and E_{peak}^{GS} is the peak energy of the gain.

We also take into account the homogeneous linewidth, arising from the dephasing processes, by supposing a Lorenzian lineshape:

$$L_{E_k}^{E_i} = \frac{\Gamma}{\pi} \frac{1}{(E_k - E_i) + \Gamma^2}.$$

where Γ is the exciton homogeneous linewidth. We have assumed a constant homogeneous linewidth of 15 meV (Sugawara et al. 2005).

The photon populations $P_{GS,ES}^{E_i}$ at GS and ES energies (normalized by the total number of QDs) are calculated as a function of energy and time, and coupled to the populations through gain and spontaneous emission terms, through the rate-equations (Markus et al. 2005):

$$\frac{dP_{GS}^{E_i}}{\partial t} = \frac{P_{GS}^{E_i}}{\tau_\varphi} + A_{GS}^{E_i} + B_{GS}^{E_i}$$
$$\frac{dP_{GS}^{E_i}}{\partial t} = \frac{P_{ES}^{E_i}}{\tau_\varphi} + 2A_{ES}^{E_i} + 2B_{ES}^{E_i}$$

and τ_ϕ is the photon life-time, considered to be 1.4 ps to allow the presence of photons in the cavity. The rates $A_{GS,ES}$ and $B_{GS,ES}$ account for the spontaneous and stimulated emission terms, respectively. To calculate these terms, it is necessary to perform a convolution of homogeneous and inhomogeneous lineshapes:

$$A_{GS,ES}^{E_i} = \frac{2\beta}{\tau_r N_D^{E_i}} \sum_{E_k} L_{E_k}^{E_i} N_D^{E_k} f_{GS,ES}^{e(E_k)} f_{GS,ES}^{h(E_k)}$$
$$B_{GS,ES}^{E_i} = 2BP_{GS,ES}^{E_i} \sum_{E_k} L_{E_k}^{E_i} N_D^{E_k} \left[f_{GS,ES}^{e(E_k)} + f_{GS,ES}^{h(E_k)} - 1\right]$$

where β is the spontaneous emission coupling factor ($\beta = 10^{-5}$) and τ_r is the radiative lifetime due to spontaneous emission ($\tau_r = 1$ ns). $f_{GS,ES}^{e,h}$ are the electron and hole distribution functions of the GS and ES. f_{WL} corresponds to the WL population divided by the total number of dots. The rate-equations for these variables are:

$$\frac{df_{GS}^{e,h(E_i)}}{dt} = \frac{2f_{ES}^{e,h(E_i)}\left[1-f_{GS}^{e,h(E_i)}\right]}{\tau_0^{e,h}} - \frac{f_{GS}^{e(E_i)}f_{GS}^{h(E_i)}}{\tau_r} - \frac{f_{GS}^{e(E_i)}f_{GS}^{h(E_i)}}{\tau_{nr}}$$
$$- \frac{f_{GS}^{e,h(E_i)}\left[1-f_{ES}^{e,h(E_i)}\right]}{\tau_{GS}^{e,h(E_i)}} - B\left[f_{GS}^{e(E_i)}+f_{GS}^{h(E_i)}-1\right]\sum_{E_k} L_{E_k}^{E_i} N_D^{E_k} P_{GS}^{E_k}$$

$$\frac{df_{ES}^{e,h(E_i)}}{dt} = \frac{f_{WL}^{e,h}\left[1-f_{ES}^{e,h(E_i)}\right]}{4\tau_c^{e,h}} - \frac{f_{ES}^{e,h(E_i)}\left[1-f_{GS}^{e,h(E_i)}\right]}{\tau_0^{e,h}} - \frac{f_{ES}^{e(E_i)}f_{ES}^{h(E_i)}}{\tau_r}$$
$$- \frac{f_{ES}^{e(E_i)}f_{ES}^{h(E_i)}}{\tau_{nr}} - \frac{f_{GS}^{e,h(E_i)}\left[1-f_{ES}^{e,h(E_i)}\right]}{2\tau_{GS}^{e,h(E_i)}} - \frac{f_{ES}^{e,h(E_i)}}{\tau_{ES}^{e,h(E_i)}}$$
$$-B\left[f_{ES}^{e(E_i)}+f_{ES}^{h(E_i)}-1\right]\sum_{E_k} L_{E_k}^{E_i} N_D^{E_k} P_{ES}^{E_k}$$

$$\frac{df_{WL}^{e,h}}{dt} = G - \frac{1}{N_D}\sum_{E_k}\frac{N_D^{E_k}\left(f_{WL}^{e,h}\left[1-f_{ES}^{e,h(E_k)}\right]\right)}{\tau_c^{e,h}} - \frac{f_{WL}^{e}f_{WL}^{h}}{\tau_r} - \frac{f_{WL}^{e}f_{WL}^{h}}{\tau_{nr}}$$
$$+\frac{1}{N_D}\sum_{E_k}\frac{4N_D^{E_k}f_{ES}^{e,h(E_k)}}{\tau_{ES}^{e,h(E_k)}}$$

where $\tau_0^{e,h}$ is the intraband relaxation time for electrons and holes. A value of $\tau_0^e = 7\,\text{ps}$ has been obtained from the ratio of GS and ES threshold currents (Markus et al. 2003), also in agreement with other previous experimental results (Sun et al. 2005). τ_0^h has been showed to be subpicosecond (Norris et al. 2005). Here we have considered a τ_0^h of 250 fs. $\tau_c^{e,h}$ is the ES capture time, 1 ps for electrons (Sun et al. 2006), subpicosecond for holes by Geller et al. (2006), for us being 0.5 ps. τ_{nr} the non-radiative life-time (arbitrarily fixed at $\tau_{nr} = 1\,\text{ns}$) and G is the carrier injection rate. Bimolecular recombination has been assumed both for radiative and for non-radiative recombination, in order to maintain charge neutrality. Indeed, for nonradiative recombination, explicitly considering an additional mid-gap level where the non-radiative processes occur would provide similar results as using bimolecular terms ($f_{GS}^e \cdot f_{GS}^h/\tau_{nr}$) as done here. The escape times from GS and ES ($\tau_{GS,ES}^{e,h(E_i)}$) are derived assuming a thermal equilibrium in the absence of external excitation (see derivation in the next section). The gain coefficient B has been fixed to get a maximum gain of $19.8\,\text{cm}^{-1}$.

The modal refractive index is calculated as a function of time through the Kramers-Kronig transform of the gain. We perform this operation by transforming the individual Lorenzian lineshapes of the dot energy intervals as done by (Gioannini et al. 2006). Considering a complex refractive index $n = \eta - i\kappa$, its real part η and imaginary part κ (accounting for gain and losses), are related by the Kramers-Kronig transform:

$$n(\omega) - 1 = \frac{2}{\pi} P \int_0^\infty \frac{E' k(E')}{E'^2 - E^2} dE'$$

where P denotes the Cauchy principal value, and E is the energy.

3 Derivation of escape times

The escape rates from the more confined towards the less confined energy levels play an important role to determine the thermal redistribution of carriers through the WL. The escape times are derived here as a function of the times associated to the inverse process of capture or relaxation, and by assuming a thermal equilibrium in the absence of external excitation. Following the approach given by Deppe and Huang (2006), we arrive to the following expressions:

$$\tau_{GS}^{e,h} = \frac{\tau_0^{e,h}}{2} exp\left(\frac{\Delta E_{ES-GS}^{e,h}}{kT}\right)$$

$$\tau_{ES}^{e,h}(E_{ES}^{i}) = \tau_c^{e,h} \frac{4N_D \pi \hbar^2}{m_r^{e,h} k_0 T} exp\left(\frac{E_{WL}^{e,h} - E_{ES}^{i}}{k_0 T}\right)$$

where ΔE_{ES-GS} is the energy difference between the GS and the ES (assumed to be 75 meV, from the spectrum, see Fig. 2), E_{WL} is the energy of the wetting layer (1.25 meV), E_{ES}^{i} is the energy of the i'th section of the ES, k_0 is the Boltzmann constant, $\hbar$ is the reduced Planck constant, m_r the reduced mass of the electrons or holes, being $0.05\,m_0$ for electrons and $0.15\,m_0$ for holes. This values are justified in (Cusack et al. 1996) and (Cusack et al. 1997). Based on energy spectra of QD amplifiers we place the GS and ES at 270 meV and 195 meV respectively from the WL. We assume that 85% of this separation corresponds to electronic levels in the conduction band and 15% to hole levels in the valence band. The resulting escape times of 95 and 30 ps for the electron escape times from the ES and GS energy peaks agree with existing experimental results (Malins et al. 2006).

As direct consequence of this energy dependence of the escape times, at low injection rates (low current) the peak gain will be centered at a lower energetic level, and it will shift to the blue as we increase the current density, as observed experimentally.

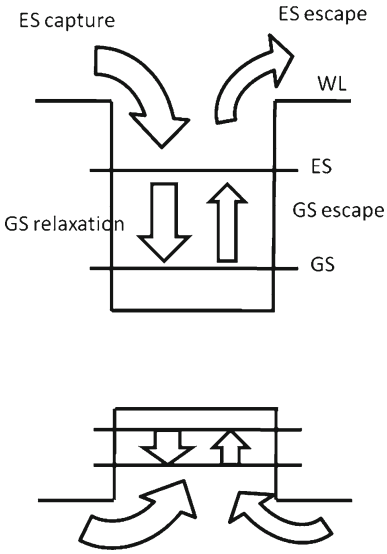

Fig. 2 Intradot mechanisms considered in the rate equations

4 Results

This model was used to simulate pump and probe experiments in QD amplifiers, i.e. the situation of interest for their use as phase modulators in all-optical Mach-Zehnder switches.

In particular, we simulate a pump and probe experiment. First, the steady-state carrier and photon populations at a certain current are calculated. Then, we perturb the steady state of the amplifier by artificially increasing the number of photons at time zero. The phase and the gain changes produced by the pump are then calculated by integrating the rate-equations.

At zero injected current, in the absorption regime, the electron energy levels are empty. When we pump optically in resonance with the gain peak, we are adding electrons and holes to the GS. These carriers will disappear initially from the GS by thermal escape to the upper levels, which is the fastest mechanism.

In Fig. 3 we see the temporal evolution of the gain at the GS peak energy. The same behavior has been reported experimentally (Cesari et al. 2007). We have separated the contribution of electrons and holes (dotted and dash-dot lines, respectively) to the gain, following the expression:

$$G_{GS}^{e,h} = \frac{1}{v_g} \sum_{E_i} 2B P_{GS}^{E_i} \sum_{E_k} L_{E_k}^{E_i} N_D^{E_k} \left[f_{GS}^{e,h(E_k)} - \frac{1}{2} \right]$$

where $G_{GS}^{e,h}$ is contribution to the total gain of the electron and hole populations.

Initially, holes will escape to the upper energetic levels by thermal escape, which is the fastest process, due to the lower energy separation of the hole energetic levels. Electron escape is a slower process taking place on the picoseconds time-scale. At longer time-scales, of the order of hundreds of picoseconds, we observe the effect of radiative and non-radiative recombinations, which depletes the carrier population with time constants of the order of nanoseconds (Zhang et al. 2000).

In Fig. 4 we represent the temporal evolution of the phase shift produced by a pump pulse resonant with the GS. We note that no phase change at GS energy is produced by a population change, at the same energy, due to the antisymmetric character of the Kramers-Kronig transform. Nevertheless, an ultrafast initial change of the phase is produced by the holes escaping to the upper levels through the ES contribution to index at the GS energy. The contribution

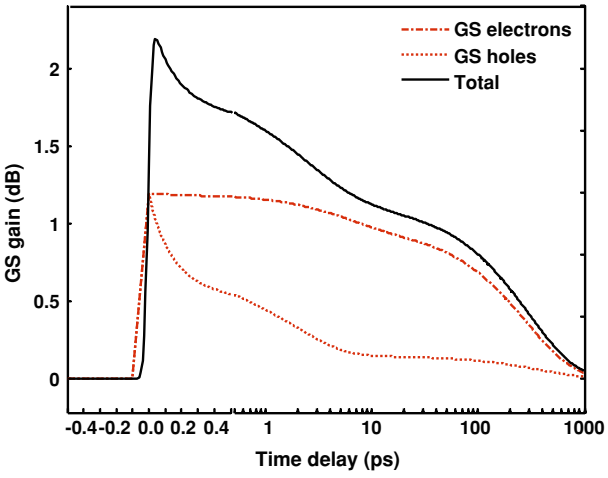

Fig. 3 Change of the gain at the GS peak after the arrival of the pump at t = 0. The current injection of the amplifier is 0 mA. The dotted line represents the contribution of the holes to the gain, which has an ultrafast decay, corresponding to the hole escape from the GS to the ES. Note that the left side is plotted in linear scale and the right side in logarithmic (x-axis). The electron contribution (dash-dot line) decays in a longer time-scale

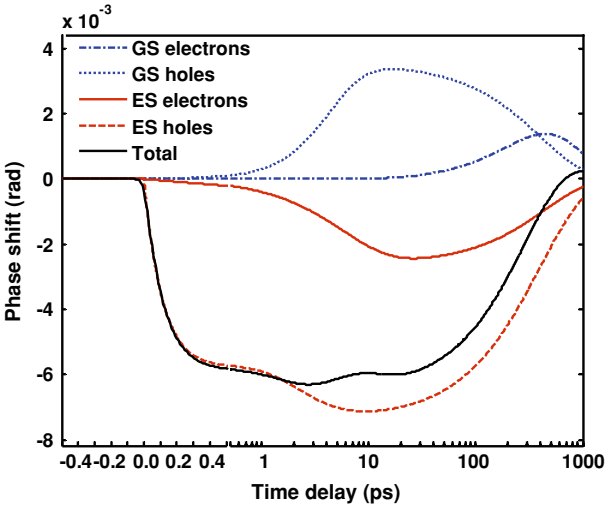

Fig. 4 Phase shift at the GS peak energy, under no injected current (0 mA). Note that the left side is plotted in linear scale and the right side in logarithmic (x-axis)

of ES carriers to the GS index was experimentally measured by Dagens et al. (2005) by the large values of the linewidth enhancement factor, and theoretically shown by Gioannini and Montrosset (2007).

The ES hole population contribution to the phase shift is represented in Fig. 4 by a dashed line. Electrons escaping from the GS will appear in the ES after some picoseconds, increasing the phase shift and slowing down the phase recovery. The contribution of the ES electrons to the phase shift is represented by a light solid line. In the 2–300 ps time scale, thermalization of GS carriers in the QD ensemble produces a non-symmetric gain change, therefore a non-zero (positive) contribution to the phase change at the GS peak energy. Interestingly, this long-lived positive phase contribution can become dominant at long time delays.

In Fig. 5 we represent the electron and hole populations as a function of the energy at different times after a perturbation (I = 0 mA). The input pulse creates electron-hole pairs at the GS energy (solid line). At this instant (t = 0), the ES is completely empty. The subsequent GS hole population decrease is due, mainly to escape to the ES. Thermal redistribution of the holes occurs after tens of ps, when holes will occupy the lower energetic levels. We observe the evolution of the energetic carrier redistribution of GS and ES from t = 1 ps (dotted line) where the shape of the perturbation still dominates, to t = 10 ps, where carriers distribute along the energetic levels as a result of the different escape times.

In contrast, electrons escape from GS to ES, but the electron population in the QD ensemble remains strongly non-thermal, due to the low escape rate to the WL. After 1 nanosecond (dot dash) most of the carriers will have abandoned the dot by means of radiative and non-radiative recombinations.

If we increase the laser current over transparency, we enter in the gain regime. The probe will be amplified, reducing the carrier population and the gain. We see the dynamics of the gain recovery in Fig. 6. The mechanisms of recovery of the gain are again different for holes and electrons. Holes (dotted line) will relax, quickly, producing a partial gain recovery in few hundreds of femtoseconds, while electrons (dot dash) will need some picoseconds as their relaxation time is longer.

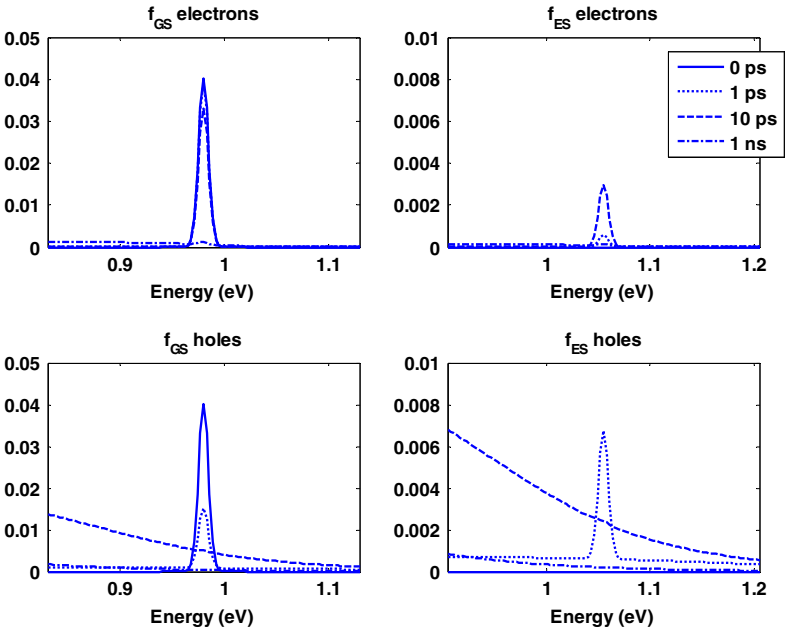

Fig. 5 Distribution functions f^{e}_{GS} (top left), f^{h}_{ES} (top right), f^{h}_{ES} (bottom left) and (bottom right) for 0 mA of current injection. The solid line represents the population just after the arrival of the pump pulse (at t = 0). At this instant, the ES is completely empty. After 1 ps (dotted line) the GS hole population starts to decrease, mainly due to escape to the ES. After 10 ps (dashed line) holes will thermally redistribute, occupying more preferably the lower energetic levels, while electrons distribution remains non-thermal. After 1 ns (dot dash) most of the carriers will have abandoned the dot by means of radiative and non-radiative recombinations

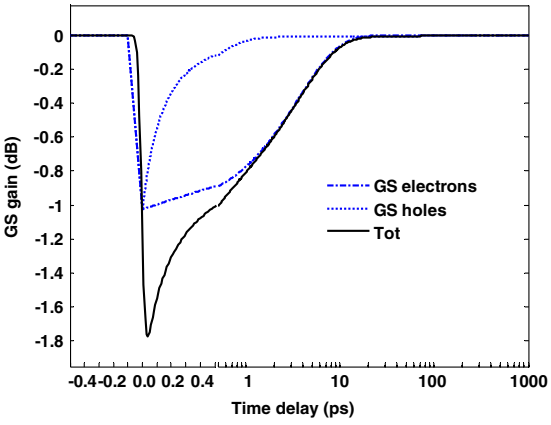

Fig. 6 Gain change produced by a resonant pump. The pump is amplified, depleting the electron and hole populations in the device, and so reducing the gain of the amplifier. A first ultrafast recovery of the gain due to hole relaxation (hole contribution is represented by a dotted line) is followed by a slower relaxation, due to the contribution of the electrons (dash-dot line). Note that the left side is plotted in linear scale and the right side in logarithmic (*x*-axis)

We note that the different escape times of electrons and holes naturally account for the two time constants observed experimentally, without the need for introducing another physical process (Auger) to explain the faster decay rates.

The phase behavior in the gain regime can also be explained with this model (Fig. 7). As holes and electrons leave the GS, they will populate the higher states. The interplay of ES to GS relaxation and WL to ES capture will describe the rise and fall of the electron

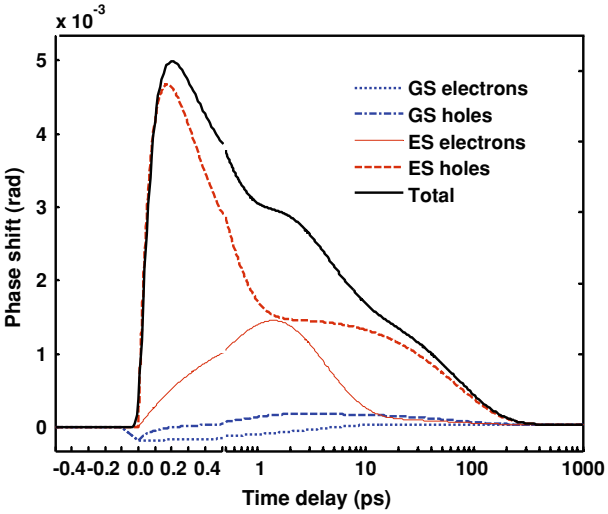

Fig. 7 Temporal evolution of the phase shift produced by the pump. The dashed line represents the contribution of the ES holes to the phase. The ultrafast initial increase is due to the hole relaxation towards the GS. The electrons of the ES (light solid line) will relax in a longer timescale (ps). In this case, the contributions of GS electrons (dotted) and GS holes (dashed) will have no effect. Note that the left side is plotted in linear scale and the right side in logarithmic (x-axis)

and hole contributions. However, the quasi-thermal ES hole population is bigger than the quasi-thermal ES electron population. This explains the long-lived hole contribution to the phase. It allows a non-negligible dephasing while the gain is already recovered, which has applications to Mach-Zehnder interferometers.

5 Conclusions

With an electron-hole rate-equations model we have given an explanation to many of the unsettled issues on the phase dynamics of QDs. The different dynamics of holes and electrons may be the reason for the appearance of two time constants. The phase shift can be high even if the gain profile is symmetric, due to the presence of carriers in the upper energetic levels. We have also shown that the phase has a slower dynamics than the gain because of the slow escape and relaxation process for the electrons.

Acknowledgements This work has been supported by the Swiss National Science Fondation and the EU-FP6 project ZODIAC, contract number FP6 (017140). We acknowledge enlightening discussions with A. Markus, P. Borri and W. Langbein.

References

Borri, P., Langbein, W., Muljarov, E.A., Zimmermann, R.: Dephasing of excited-state excitons in InGaAs quantum dots. Physica Status Solidi B-Basic Solid State Phys. **243**, 3890–3894 (2006)

Cesari, V., Langbein, W., Borri, P., Rossetti, M., Fiore, A., Mikhrin, S., Krestnikov, I., Kovsh, A.: Ultrafast gain dynamics in 1.3 µm InAs/GaAs quantum-dot optical amplifiers: The effect of p doping. Appl. Phys. Lett. **90**(20), 201103 (2007)

Cusack, M., Briddon, P., Jaros, M.: Electronic structure of InAs/GaAs self-assembled quantum dots. Phys. Rev. B **54**(4), R2300–R2303 (1996)

Cusack, M., Briddon, P., Jaros, M.: Absorption spectra and optical transitions in InAs/GaAs self-assembled quantum dots. Phys. Rev. B **56**(7), 4047–4050 (1997)

Dagens, B., Markus, A., Chen, J.X., Provost, J.-G., Make, D., Le Gouezigou, O., Landreau, J., Fiore, A., Thedrez, B.: Giant linewidth enhancement factor and purely frequency modulated emission from quantum dot lasers. IEE Electron Lett. **41**(6), 323–324 (2005)

Dawson, P., Rubel, O., Baranovskii, S., Pierz, K., Thomas, P., Gobel, E.: Temperature-dependent optical properties of InAs/GaAs quantum dots: Independent carrier versus exciton relaxation. Phys. Rev. B **72**(23), 235301 (2005)

Deppe, D., Huang, H.: Fermi's golden rule, nonequilibrium electron capture from the wetting layer, and the modulation response in P-doped quantum-dot lasers. IEEE J. Quant. Electron **42**(3), 324–330 (2006)

Fathpour, S., Mi, Z., Bhattacharya, P., Kovsh, A., Mikhrin, S., Krestnikov, I., Kozhukhov, A., Ledentsov, N.: The role of Auger recombination in the temperature-dependent output characteristics (T-0 = infinity) of p-doped 1.3 µm quantum dot lasers. Appl. Phys. Lett. **85**(22), 5164–5166 (2004)

Geller, M., Marent, A., Stock, E., Bimberg, D., Zubkov, V., Shulgunova, I., Solomonov, A.: Hole capture into self-organized InGaAs quantum dots. Appl. Phys. Lett. **89**(23), 232105 (2006)

Gioannini, M., Sevega, A., Montrosset, I.: Simulations of differential gain and linewidth enhancement factor of quantum dot semiconductor lasers. Opt. Quant. Electron **38**, 381–394 (2006)

Gioannini, M., Montrosset, I.: Numerical analysis of the frequency chirp in quantum-dot. Semiconductor Lasers **43**(10), 941–949 (2007)

Malins, D., Gomez-Iglesias, A., White, S., Sibbett, W., Miller, A., Rafailov, E.: Ultrafast electroabsorption dynamics in an InAs quantum dot saturable absorber at 1.3 µm. Appl. Phys. Lett. **89**(17), 171111 (2006)

Markus, A., Chen, J., Paranthoen, C., Fiore, A., Platz, C., Gauthier-Lafaye, O.: Simultaneous two-state lasing in quantum-dot lasers. Appl. Phys. Lett. **82**(12), 1818 (2003)

Markus, A., Rossetti, M., Calligari, V., Chen, J., Fiore, A.: Role of thermal hopping and homogeneous broadening on the spectral characteristics of quantum dot lasers. J. Appl. Phys. **98**(10), 104506 (2005)

Narvaez, G., Bester, G., Zunger, A.: Carrier relaxation mechanisms in self-assembled (In,Ga)As/GaAs quantum dots: Efficient P → S Auger relaxation of electrons. Phys. Rev. B **74**(7), 075403 (2006)

Norris, T.B., Kim, K., Urayama, J., Wu, K.Z., Singh, J., Bhattacharya, P.K.: Density and temperature dependence of carrier dynamics in self-organized InGaAs quantum dots. J. Phys. D-Appl. Phys. **38**(13), 2077–2087 (2005)

O'Driscoll, I., Piwonski, T., Schleussner, C.-F., Houlihan, J., Huyet, G., Manning, R.J.: Electron and hole dynamics of InAs/GaAs quantum dot semiconductor optical amplifiers. Appl. Phys. Lett. **91**(7), 071111 (2007)

Piwonski, T., O'Driscoll, I., Houlihan, J., Huyet, G., Manning, R., Uskov, A.: Carrier capture dynamics of InAs/GaAs quantum dots. Appl. Phys. Lett. **90**(12), 122108 (2007)

Rossetti, M., Markus, A., Fiore, A., Occhi, L., Vélez, C.: Quantum dot superluminescent diodes emitting at 1.3 µm. IEEE Photonics Technol. Lett. **17**(3), 540–542 (2005)

Saito, H., Nishi, K., Kamei, A., Sugou, S.: Low chirp observed in directly modulated quantum dot lasers. IEEE Photonics Technol. Lett. **12**(10), 1298–1300 (2000)

Sugawara, M., Hatori, N., Ebe, H., Ishida, M., Arakawa, Y., Akiyama, T., Otsubo, K., Nakata, Y.: Modeling room-temperature lasing spectra of 1.3-µm self-assembled InAs/GaAs quantum-dot lasers: Homogeneous broadening of optical gain under current injection. J. Appl. Phys. **38**(13), 2126–2134 (2005)

Sun, K., Chen, J., Lee, B., Lee, C., Kechiantz, A.: Carrier capture and relaxation in InAs quantum dots. Nanotechnology **16**, 1530–1535 (2005)

Sun, K., Kechiantz, A., Lee, B., Lee, C.: Ultrafast carrier capture and relaxation in modulation-doped InAs quantum dots. Appl. Phys. Lett. **88**(16), 163117 (2006)

van der Poel, M., Gehrig, E., Hess, O., Birkedal, D., Hvam, J.: Ultrafast gain dynamics in quantum-dot amplifiers: Theoretical analysis and experimental investigations. IEEE J. Quant. Electron **41**(9), 1115–1123 (2005)

Viktorov, E., Mandel, P., Tanguy, Y., Houlihan, J., Huyet, G.: Electron-hole asymmetry and two-state lasing in quantum dot lasers. Appl. Phys. Lett. **87**(5), 053113 (2005)

Zhang, L., Boggess, T., Deppe, D., Huffaker, D., Shchekin, O., Cao, C.: Dynamic response of 1.3-µm-wavelength InGaAs/GaAs quantum dots. Appl. Phys. Lett. **76**(10), 1222–1224 (2000)